Flow of Micropolar–Newtonian Fluids through the Composite Porous Layered Channel with Movable Interfaces

Sneha Jaiswal[1] · Pramod Kumar Yadav[1]

Abstract

In this work, we have discussed the effect of width of the layers on the micropolar–Newtonian fluid flow through the porous layered rectangular pipe. The mathematical model of our problem represents the sandwiching of non-Newtonian fluid between the Newtonian fluid layers. The horizontal porous channel is divided into three porous layers with different permeabilities, and the problem is modeled in such a way that the width of each layer can be varied. The flow in the respective porous region took place due to the constant pressure gradient along the direction of the flow. Brinkman equation has been used for the fluids flowing through the porous medium. The problem is solved analytically, and the expressions for the flow velocity, volumetric flow rate and shearing stresses at the walls of the horizontal plates are obtained in the closed form. The impact of width of the middle porous layer is seen on the mean flow velocity, velocity profile, interfacial velocities and interfacial shear stresses. The present work has a setup that will be useful in oil recovery process, filtration of the contaminated ground water and some medical purposes.

Keywords Micropolar fluid · Interface · Porous medium · Darcy number · Micropolarity parameter

1 Introduction

With the advent of time, the study of fluid mechanics is emerging as a great challenge for the researchers and scientists. The advances in the fluid mechanics are increasing because of the dependency of our life on the fluids. The air that we breathe, the fluid and food which we take for living, and the motion of physiological fluids and industrial fluids are some very well-known examples to express the importance of fluid mechanics [1]. Dealing with the real-life problems, the mediums which transmit the fluids are of great importance in the work of fluid flow problems. One of such media is the porous materials which consist of some voids and solids spaces [2]. The water and food transportation to the plants, recovery of the oils from earth layers, filtrations of the contaminated water, etc. are the examples of fluid flow through porous media. Yadav et al. [3–5] solved the problems of the porous membrane comprising of spherical/ spheroidal particles, using cell model technique.

The process of extracting petrol/oils from the porous earth layers and recovery of groundwater, body fluids through the tissues and blood through arteries require the knowledge of fluid flow through the rectangular geometry occupied by porous medium. Such topics are grabbing attention of many researchers, industrialists, geologist and various scientists because of its lot of applications. Viewing the various applications, Hamdan [6] reported a review paper on the single-phase flow through the porous channel with the discussion involving various mathematical models. Rudraiah [7] derived the slip condition for the Poiseuille–Couette flow between two parallel plates, bounding porous material. Kaviany [8] considered the convective and boundary effects for channel flow and concluded that the velocity variation strictly depends on the porous medium shape parameter. Chamkha [9] solved the hydromagnetic fully developed laminar mixed convection fluid flow problem and discussed the problem in the presence or absence of heat generation or absorption effects. Numerous works on the flow and heat transfer through the channel filled with porous medium are done by Umavathi et al. [10–13] and Chamkha et al. [14]. Ismael et al. [15] solved numerically the steady laminar mixed convection flow problem for a lid-driven square cavity filled with the water. Chamkha [16] did an analysis on the unsteady,

✉ Sneha Jaiswal
  snehajwl10@gmail.com

1 Department of Mathematics, Motilal Nehru National Institute of Technology Allahabad, Prayagraj 211004, India

laminar double-diffusive convective flow of a binary gas mixture through the porous medium. Magyari and Chamkha [17] investigated the steady laminar magnetohydrodynamic thermosolutal Marangoni convection in the boundary layer approximation. The problem of Newtonian fluid past through the identical cylindrical shells was solved by Yadav [18] using particle-in-cell method. Tiwari et al. [19] analyzed the creeping flow through membrane of non-homogeneous porous cylindrical particles using Darcy law. They studied the effects of various parameters on membrane's permeability. Vafai and Thiyagaraja [20] done analysis on the flow and heat transference for the three types of the interfacial region of porous medium and solved the problem by analytical as well as numerical method. Sahraoui and Kaviany [21] considered the slip and no-slip boundary conditions at the interface of porous and plain medium and investigated the parameters on which the slip coefficient relies.

As work proceeded in the direction of involving as much as real-life problems, the researchers started working with the immiscible fluids through the different regimes of porous layers. Ansari and Deo [22] observed the magnetic field effect on the channel flow of two Newtonian fluids of different viscosities. The unsteady flow and heat transfer of two-fluid system discussed with useful results in the works [23–26]. Umavathi et al. [27] analyzed the problem of fully developed flow of two immiscible viscous and couple stress fluids through composite porous medium. An unsteady laminar magnetohydrodynamic flow and heat transfer of a particulate suspension in an electrically conducting fluid through channels and circular pipes are discussed by Chamkha [28]. Allan and Hamdan [29] discussed the model of fluid flow with two different layers of porous medium in which one of the porous regions is governed by Brinkman and another by Forchheimer equation. In this work, they evaluated the interfacial velocity and discussed its dependency on the Darcy numbers. Ford and Hamdan [30] solved the problem on the porous layers having different permeabilities and used the finite difference scheme to obtain the solutions of the flow models. Recently, Yadav [31] have discussed the motion of the fluid flow through the porous membrane of variable permeability. Hamdan et al. [32] studied the Poiseuille flow through the porous channel considering different permeability functions. The problem of 2-D fully developed Stokes flow passing through horizontal porous pipe was solved by Awartani and Hamdan [33]. In this paper, they discussed about three types of flows that were the Poiseuille flow, Couette flow and Poiseuille–Couette flow, respectively. Chandersis and Jamet [34] investigated the boundary condition for the fluid–porous interface and solved the problem using method of asymptotic expansions.

The transition layer in the fluid flow through the different layers plays an important role in various applications. Nield and Kuznetsov [35] modeled the Newtonian fluid flow in three layers of horizontal channel and observed the transition layer's effect on the motion of fluid at different Darcy numbers. Umavathi et al. [36] considered fully developed flow and heat transfer of couple stress fluid sandwiched between two Newtonian fluids in the horizontal channel and solved the problem analytically. Zaytoon et al. [37, 38] used same model but with different permeability functions for the transition layer. In both the works, they solved the Brinkman equation by reducing it into the Airy's differential equation. Zaytoon et al. [39] modeled the Newtonian fluid flow through porous medium of finite or infinite thickness in a horizontal channel and solved the problem by using Darcy equation for the porous region having variable permeability. Zaytoon et al. [40] extended their previous work by considering Brinkman layer sandwiched between two Darcy layers, and the problem was solved using Airy's function and Nield–Kuznetsov function. Alzahrani et al. [41] gave a note on the flow through porous medium having variable permeability and the fluid having pressure-dependent viscosity; they had considered the porous material inside an inclined channel. Umavathi et al. [42] solved the problem in which the middle layer is occupied by micropolar fluid and the width of the three layers is fixed and equal. A similar type of work on the heat transfer and flow of micropolar fluid can be found in the works [43–46].

The wide scope of fluid flow through different permeabilities of porous layers occurs in the oil reservoirs, in groundwater recovery and in blood flow through different layers of arteries. Various significant investigations were conducted, and the results are obtained for the model of immiscible fluids. Yadav et al. [47] discussed the application and motivation for the flow of micropolar–Newtonian fluids through porous channel and presented the effect of various parameters on the flow. Later on, Yadav et al. [48] investigated the presence of inclined magnetic field on the micropolar–Newtonian flow model. One of our recent works [49] dealt with the stratified flow of immiscible Newtonian–micropolar–Newtonian fluids with fixed interfaces. Saad et al. [50] discussed the model for immiscible CO_2–oil and concluded that the model plays significant role in oil displacement process. Flow of non-Newtonian and Newtonian fluids through porous medium rigorously occurs in the petroleum industries. Siddique et al. [51] discussed experimentally and numerically the model of crude oil and water. Being motivated by the above-discussed literatures, mostly [37–41] and various applications [50, 51], we decided to discuss the present problem.

In the present work, the model is chosen in a way that horizontal channel is divided into three different porous regions and the widths of each region can be varied. The micropolar fluid is assumed to flow in the middle porous layer of the channel. Though our present model resembles with our previous work [49], the problem discussed here is considerably different. Previously we fixed the width of each porous layer of the horizontal channel, while here

the interfaces are movable, i.e., they can be varied accordingly to the need. Also, here we have taken each porous layer of different permeabilities and presented the effect of three different Darcy numbers on the flow and Brinkman transition layer via graphs and tables, in the absence of magnetic field. Although some authors such as Zaytoon et al. [37, 38] have solved the problem on movable interface by considering Newtonian fluid sandwiched between the Newtonian fluid layers, here, we consider non-Newtonian fluid sandwiched between the Newtonian fluid porous layers with movable interfaces. Our objective in this work is to present the effect of width of micropolar fluid layer sandwiched between two Newtonian fluid layers on the stresses at the interfaces, velocities of fluids and on the different Darcy numbers of the porous layers. Since a mathematical model for the oil recovery process plays an important role in the enhancement process, our model can be widely used for the oil extraction process. Such type of model is important in various industrial and natural applications [35, 37–40] that deal with the ground water recovery; recovery of oil and gas; designing of cooling and heating systems; flow of oil through the porous rock layers; the flow of nutrients and water into plants branches; blood flow in animal/human body tissues; lubrication mechanisms; design of aircraft wings with porous nature to lessen the drag force; and study of fuel cells depending on an analysis of fluid flow through and over porous medium layers.

2 Formulation of the Problem

2.1 Mathematical Model

The schematic representation of model for the concerned problem is shown in Fig. 1. The horizontal channel is formed by two parallel solid plates at $y = h$ and $y = 0$, respectively. The channel is filled with three layers of the porous medium of different permeabilities: k_1, k_2 and k_3. The three layers of the porous medium in the horizontal channel are modeled in such a way that the width of each layer can be varied. The widths of region-I ($h \leq y \leq \beta h$), region-II ($\beta h \leq y \leq \alpha h$) and region-III ($0 \leq y \leq \alpha h$) from the top to bottom are $(1 - \beta)h$, $(\beta - \alpha)h$ and αh, respectively.

The values of α and β are chosen in such a way that the middle layer can be thicker, thinner and of equal width with respect to the other layers. The Newtonian fluid is allowed to flow in the upper and lower porous regions of the channel, respectively, and micropolar fluid in region-II, i.e., region which is sandwiched between the Newtonian fluids. The fluids, which are flowing through the horizontal porous channel, are assumed to be steady and incompressible. It is also assumed that the flow is fully developed, i.e., no variation in the flow velocity along the direction of flow. The flow through the composite porous layers takes place due to constant pressure gradient along the direction of flow.

2.2 Description of the Governing Equations

In 1947, Brinkman [52] did a remarkable work for the fluid flow through porous medium of high permeability. He extended the Darcy law [53] by adding viscous term. As we are considering the flows through porous medium of high permeability, the Brinkman equation [52] for the Newtonian fluids (in the absence of any external forces) is described below:

$$\text{grad}\, p = -\frac{\mu}{k}\mathbf{v} + \mu_{\text{eff}}\Delta\mathbf{v}, \tag{1}$$

where p is the pressure gradient and k is the permeability of the porous medium. Here, μ and μ_{eff} are viscosity and effective viscosity of the fluid, respectively, and $\mathbf{v}$ is the flow velocity of the fluid. Liu and Masliyah [54] discussed the

Fig. 1 Representation of the model
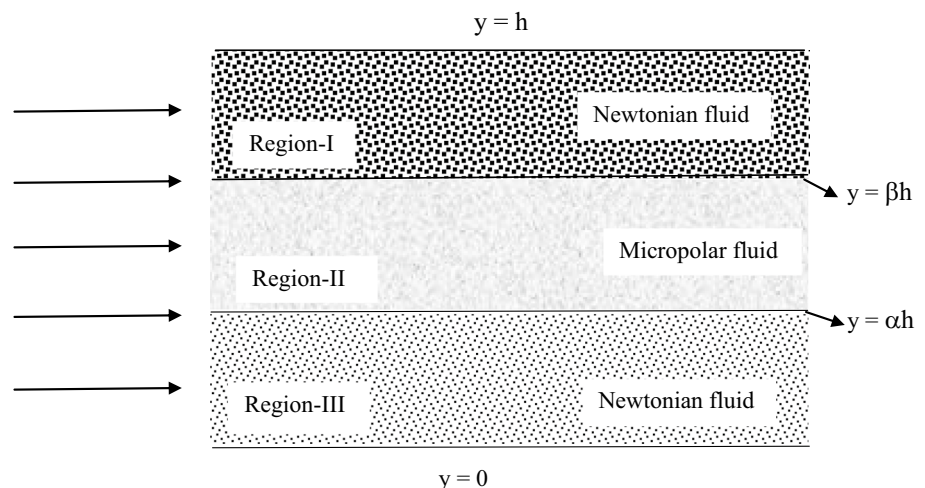
relation between effective viscosity μ_{eff} and viscosity of fluid μ and concluded that the relation between effective viscosity μ_{eff} and viscosity of fluid μ depends on the types of porous media, i.e., effective viscosity of fluid in porous region may either greater or smaller than the viscosity of fluid. Nield and Bejan [55] had provided an important conclusion in his work that both μ_{eff} and μ are equal for high porosity. Let the velocity components of Newtonian fluid with same viscosity in region-I and region-III of the horizontal porous channel be $(u_1, 0, 0)$ and $(u_3, 0, 0)$, respectively. It is important to note that the y-component of velocity becomes constant because of the fully developed flow and continuity equation for incompressible flow; and this component vanishes when we apply the no-slip boundary condition at the parallel plates. Fully developed flow condition suggest that the x-components of velocities u_1 *and* u_3 will be function of y only, i.e., $u_1 = u_1(y)$ and $u_3 = u_3(y)$. The permeability of the respective regions is assumed as k_1 and k_3. Thus, the equations governing the flows in the region-I and region-III are given as:

Region-I

$$\mu_1 \frac{d^2 u_1}{dy^2} - \frac{\mu_1}{k_1} u_1 - \frac{dp}{dx} = 0, \tag{2}$$

where μ_1 is the viscosity of the fluid which is taken same as the effective viscosity of fluid. Similarly, the equation for the region-III is mentioned below:

Region-III

$$\mu_1 \frac{d^2 u_3}{dy^2} - \frac{\mu_1}{k_3} u_3 - \frac{dp}{dx} = 0. \tag{3}$$

The theory of micropolar fluid, which is flowing through the middle layer of the horizontal porous channel, was introduced by Eringen [56, 57]. Micropolar fluid is a kind of a non-Newtonian fluid characterized by the local motion of its constituents' particles; it deals with the non-symmetric stress and couple stress tensor. Fluids exhibiting such rotational motion of its particles and following the respective constitutive equation are known to be micropolar fluid, for example liquid crystals, animal blood, body fluids, polymers, etc. The field equations [58] for the micropolar fluid are described below:

$$\frac{\partial \rho}{\partial t} + \nabla \cdot (\rho \mathbf{v}) = 0, \tag{4}$$

$$\rho \frac{D\mathbf{v}}{Dt} = -\nabla p + (\lambda + \mu - \mu_r)\nabla \text{div}\mathbf{v} + (\mu + \mu_r)\Delta \mathbf{v} + 2\mu_r \nabla \times \boldsymbol{\omega} + \rho f, \tag{5}$$

$$\rho I \frac{D\boldsymbol{\omega}}{Dt} = 2\mu_r(\nabla \times \mathbf{v} - 2\boldsymbol{\omega}) + (c_0 + c_d - c_a)\nabla \text{div}\boldsymbol{\omega} + (c_a + c_d)\Delta \boldsymbol{\omega} + \rho g, \tag{6}$$

where λ and μ are the viscosity coefficients; μ_r denotes the dynamic microrotational viscosity; c_0, c_d, c_a are known as coefficients of angular viscosities. Here, I, f and g represent microinertia coefficient, external linear and couple forces, respectively. The linear and microrotational velocity of the micropolar fluid is denoted by $\mathbf{v}$ and $\boldsymbol{\omega}$, respectively. Using Eqs. (4)–(6) and Eq. (1), the equation for the micropolar fluid passing through middle porous layer, i.e., $(\beta h \leq y \leq \alpha h)$ of the horizontal channel is given as:

Region-II $(\beta h \leq y \leq \alpha h)$

$$(\mu + \kappa)\frac{d^2 u_2}{dy^2} + \kappa \frac{d\omega}{dy} - \frac{\mu}{k_2} u_2 - \frac{dp}{dx} = 0, \tag{7}$$

$$\gamma \frac{d^2 \omega}{dy^2} - \kappa \left(2\omega + \frac{du_2}{dy} \right) = 0. \tag{8}$$

Here μ, κ and γ are the viscosity coefficients of micropolar fluid. The component form of linear and microrotational velocities is $(u_2, 0, 0)$ and $(0, 0, \omega)$, respectively.

The mathematical expression for γ is used by Ahmadi et al. [59] is as follows:

$$\gamma = \left(\mu + \frac{\kappa}{2} \right) j,$$

where $j = h^2$ is known to be microinertia density.

3 Solution of the Problem

Equations (2), (3), (7) and (8) are made dimensionless by considering the following parameters:

$$\tilde{u}_i = \frac{u_i}{U}, \ \tilde{y} = \frac{y}{h}, \ \tilde{x} = \frac{x}{h}, \ \tilde{p} = \frac{p}{\mu_1 U/h},$$
$$\tilde{\omega} = \frac{\omega}{U/h}, \ Da_i = \frac{k_i}{h^2} \text{ and } m = \frac{\mu_1}{\mu}. \tag{9}$$

Here U and h represent the characteristic velocity and length, respectively. The symbol $Da_i, \ i = 1, 2, 3,$ represents the Darcy number in the respective porous region. The maximum value of Darcy numbers can be unity as discussed in the work of Zaytoon et al. [37–40].

With the use of Eq. (9), the non-dimensional form of (dropping tilde) Eqs. (2), (3), (7) and (8) can be written as:

Region-I $(\beta \leq y \leq 1)$

$$\frac{d^2 u_1}{dy^2} - \frac{u_1}{Da_1} = P, \tag{10}$$

where Da_1 is the Darcy number for porous region-I and $P = \frac{dp}{dx}$ is the constant pressure gradient.

Region-II ($\alpha \leq y \leq \beta$)

$$(1 + K)\frac{d^2 u_2}{dy^2} + K\frac{d\omega}{dy} - \frac{u_2}{Da_2} = mP, \tag{11}$$

$$\left(1 + \frac{K}{2}\right)\frac{d^2\omega}{dy^2} - K\left(2\omega + \frac{du_2}{dy}\right) = 0, \tag{12}$$

where $K = \frac{\kappa}{\mu}$, which is known as the material parameter of Eringen/micropolar fluid. On putting $K = 0$, the field equations of micropolar fluid will become uncoupled and reduces to the classical Navier–Stokes equation for Newtonian fluids. The range of values of micropolar parameter is $K \in [0, \infty)$ which is discussed in the work of Eringen [57]. Here, the Darcy number for the middle layer is denoted by Da_2.

Region-III ($\alpha \leq y \leq 0$)

$$\frac{d^2 u_3}{dy^2} - \frac{u_3}{Da_3} = P, \tag{13}$$

where Da_3 is the Darcy number for the lower porous layer of the horizontal channel.

Equation (10) can be solved directly by the classical method of solving linear differential equation. Let $\lambda_1 = \frac{1}{\sqrt{Da_1}}$, then Eq. (10) can be rewritten as:

$$(D^2 - \lambda_1^2)u_1 = P, \tag{14}$$

where D^2 represents the second differential operator. Thus, the velocity of Newtonian fluid in the region-I is given as:

$$u_1(y) = C_1 \exp(\lambda_1 y) + C_2 \exp(-\lambda_1 y) - \frac{P}{\lambda_1^2}. \tag{15}$$

Similarly, the velocity of Newtonian fluid in the region-III becomes as follows:

$$u_3(y) = C_7 \exp(\lambda_3 y) + C_8 \exp(-\lambda_3 y) - \frac{P}{\lambda_3^2}, \tag{16}$$

where $\lambda_3 = \frac{1}{\sqrt{Da_3}}$.

Equations (11) and (12) are the coupled differential equations, and the linear and microangular velocity of micropolar fluid can be found by solving Eqs. (11) and (12) together.

The linear and microangular motions of the micropolar fluid in the middle porous layer are having the following expressions:

$$u_2(y) = C_3 \exp(\eta y) + C_4 \exp(-\eta y) + C_5 \exp(\xi y) + C_6 \exp(-\xi y) - \frac{mP}{\lambda_2^2}, \tag{17}$$

$$\omega(y) = S[C_3 \exp(\eta y) - C_4 \exp(-\eta y)] + T[C_5 \exp(\xi y) - C_6 \exp(-\xi y)], \tag{18}$$

where $\eta = \sqrt{\frac{h^2 + \sqrt{h^4 - 4k^2}}{2}}$, $\xi = \sqrt{\frac{h^2 - \sqrt{h^4 - 4k^2}}{2}}$, $h^2 = \frac{2K + \lambda_2^2}{(1+K)}$, $k^2 = \frac{4K\lambda_2^2}{(2+K)(1+K)}$,

$$S = \frac{(2+K)\lambda_2^2\eta}{4K^2} - \frac{\eta}{2} - \frac{(1+K)(2+K)\eta^3}{4K^2} \text{ and}$$

$$T = \frac{(2+K)\lambda_2^2\xi}{4K^2} - \frac{\xi}{2} - \frac{(1+K)(2+K)\xi^3}{4K^2}$$

In the expression of the flow velocities, Eqs. (15)–(18) involved eight arbitrary constants C_1, C_2, C_3, C_4, C_5, C_6, C_7 and C_8. The mathematically consistent and reliable boundary and interface conditions can be used to get the values of these arbitrary constants. The boundary conditions which are used at the boundaries and interfaces are discussed in the next section.

3.1 Boundary Conditions

In this section, we have given the conditions at boundaries and interfaces in non-dimensional forms.

Zero-velocity boundary conditions at solid walls:

$$u_1 = 0 \text{ at } y = 1, \tag{19}$$

$$u_3 = 0 \text{ at } y = 0. \tag{20}$$

The tangential velocities are continuous at the interfaces $y = \beta$ and $y = \alpha$:

$$u_1(\beta) = u_2(\beta), \tag{21}$$

$$u_2(\alpha) = u_3(\alpha). \tag{22}$$

The continuity in shearing stresses at the interfaces $y = \beta$ and $y = \alpha$:

$$m\frac{du_1}{dy}\bigg|_{y=\beta} = (1 + K)\frac{du_2}{dy}\bigg|_{y=\beta} + K\omega(\beta), \tag{23}$$

$$(1 + K)\frac{du_2}{dy}\bigg|_{y=\alpha} + K\omega(\alpha) = m\frac{du_3}{dy}\bigg|_{y=\alpha}. \tag{24}$$

The constant cell rotational velocity at the interfaces $y = \beta$ and $y = \alpha$:

$$\frac{d\omega}{dy}\bigg|_{y=\beta} = 0, \tag{25}$$

$$\frac{d\omega}{dy}\bigg|_{y=\alpha} = 0. \tag{26}$$

3.2 Determination of the Arbitrary Constants

On substituting the boundary conditions from Eqs. (19)–(26) into Eqs. (13), (16), (17) and (18), we obtained the system of algebraic equations (linear in nature) for the corresponding constants arising in the solution of the velocities. The system of equations is written in matrix form as follows:

$$AX = B, \tag{27}$$

where

$$A = \begin{bmatrix} e^{\lambda_1} & e^{\lambda_1} & 0 & 0 & 0 & 0 & 0 & 0 \\ 0 & 0 & 0 & 0 & 0 & 0 & 1 & 1 \\ e^{\lambda_1\beta} & e^{-\lambda_1\beta} & -e^{\eta\beta} & -e^{-\eta\beta} & -e^{\xi\beta} & -e^{-\xi\beta} & 0 & 0 \\ 0 & 0 & e^{\eta\alpha} & e^{-\eta\alpha} & e^{\xi\alpha} & e^{-\xi\alpha} & -e^{\lambda_3\alpha} & -e^{-\lambda_3\alpha} \\ m\lambda_1 e^{\lambda_1\beta} & m\lambda_1 e^{\lambda_1\beta} & -Le^{\eta\beta} & Le^{-\eta\beta} & -Me^{\xi\beta} & Me^{-\xi\beta} & 0 & 0 \\ 0 & 0 & Le^{\eta\alpha} & -Le^{-\eta\alpha} & Me^{\xi\alpha} & -Me^{-\xi\alpha} & -m\lambda_3 e^{\lambda_3\alpha} & -m\lambda_3 e^{-\lambda_3\alpha} \\ 0 & 0 & S\eta e^{\eta\beta} & S\eta e^{-\eta\beta} & T\xi e^{\xi\beta} & T\xi e^{-\xi\beta} & 0 & 0 \\ 0 & 0 & S\eta e^{\eta\alpha} & S\eta e^{-\eta\alpha} & T\xi e^{\xi\alpha} & T\xi e^{-\xi\alpha} & 0 & 0 \end{bmatrix},$$

$$X = \begin{bmatrix} C_1 & C_2 & C_3 & C_4 & C_5 & C_6 & C_7 & C_8 \end{bmatrix}^T,$$

$$B = \begin{bmatrix} \frac{P}{\lambda_1^2} & \frac{P}{\lambda_3^2} & \frac{P}{\lambda_1^2} - \frac{mP}{\lambda_2^2} & -\frac{P}{\lambda_3^2} + \frac{mP}{\lambda_2^2} & 0 & 0 & 0 & 0 \end{bmatrix}^T,$$

$$L = [\eta(1 + K) + SK], \quad M = [\xi(1 + K) + TK].$$

Solving matrix given by (27) (with the use of Mathematica 10.3), the authors have obtained the values of the constants C_1, C_2, C_3, C_4, C_5, C_6, C_7 and C_8. Since these values are cumbersome, we refrain from presenting the values in the manuscript.

Inserting the values of the above arbitrary constants in Eqs. (15), (16), (17) and (18), we can obtain the velocity of micropolar–Newtonian fluids in their respective regions, i.e., we obtained the values of $u_1(y)$, $u_2(y)$, $\omega(y)$ and $u_3(y)$.

The tangential velocity at the two interfaces, i.e., at $y = \alpha$ and $y = \beta$ is given as:

$$u_1(\beta) = C_1 \exp(\lambda_1\beta) + C_2 \exp(-\lambda_1\beta) - \frac{P}{\lambda_1^2}, \tag{28}$$

$$u_3(\alpha) = C_7 \exp(\lambda_3\alpha) + C_8 \exp(-\lambda_3\alpha) - \frac{P}{\lambda_3^2}, \tag{29}$$

where the arbitrary constants C_1, C_2, C_7 and C_8 already have been evaluated. Hence, we can find the expression for tangential velocity at the interfaces.

4 Volumetric Flow Rate and Stresses

4.1 Evaluation of Volumetric Flow Rate

The non-dimensional volume flux through the horizontal porous layers is given as:

$$Q = \int_0^\alpha u_3(y)\mathrm{d}y + \int_\alpha^\beta u_2(y)\mathrm{d}y + \int_\beta^1 u_1(y)\mathrm{d}y. \tag{30}$$

Using the values of velocities from Eqs. (15), (16) and (17) in (30), we can get the flow rate which is given below:

$$\begin{aligned} Q = & \frac{1}{\lambda_3}\left[C_7\{\exp(\lambda_3\alpha) - 1\} - C_8\{\exp(-\lambda_3\alpha) - 1\} - \frac{P\alpha}{\lambda_3}\right] \\ & + \frac{1}{\eta}\left[C_3\{\exp(\eta\beta) - \exp(\eta\alpha)\} - C_4\{\exp(-\eta\beta) - \exp(-\eta\alpha)\}\right] \\ & + \frac{1}{\xi}\left[C_5\{\exp(\xi\beta) - \exp(\xi\alpha)\} - C_6\{\exp(-\xi\beta) - \exp(-\xi\alpha)\}\right] \\ & - \frac{mP}{\lambda_2^2}(\beta - \alpha) \\ & + \frac{1}{\lambda_1}\left[C_1\{\exp(\lambda_1) - \exp(\lambda_1\beta)\} - C_2\{\exp(\lambda_1) - \exp(\lambda_1\beta)\} - \frac{P(1 - \beta)}{\lambda_1}\right]. \end{aligned} \tag{31}$$

4.2 Evaluation of Shear Stress at the Porous Interface

The shear stresses at the upper and lower interfaces of the porous layers, i.e., τ_β and τ_α, respectively, in non-dimensional form are given below:

$$\tau_\beta = \left(\frac{\mathrm{d}u_1}{\mathrm{d}y}\right)_{y=\beta}, \tag{32}$$

$$\tau_\alpha = \left(\frac{\mathrm{d}u_3}{\mathrm{d}y}\right)_{y=\alpha}. \tag{33}$$

Using the values of velocities in Eqs. (32)–(33), we can obtain the expression of shear stresses at the upper and lower interfaces of the porous layers which are given below

$$\tau_\beta = C_1\lambda_1 \exp(\lambda_1\beta) - C_2\lambda_1 \exp(-\lambda_1\beta), \tag{34}$$

$$\tau_\alpha = C_7\lambda_3 \exp(\lambda_3\alpha) - C_8\lambda_3 \exp(-\lambda_3\alpha). \tag{35}$$

5 Results and Discussion

In the present work, our main objective is to present the effect of micropolar fluid layer on fluid flow quantities that describe the motion of the fluids like flow velocity, flow rate, shear stress, etc. To observe the effect, we have chosen the width of middle layer in the following manner:

(a) When middle layer is thicker than the other porous layers, i.e., when $\alpha = 1/4$ and $\beta = 3/4$.
(b) When middle layer is thinner than the other porous layers, i.e., when $\alpha = 0.49$ and $\beta = 0.51$.

(c)   When width of the middle layer is same as the width of the other porous layers, i.e., when $\alpha = 1/3$ and $\beta = 2/3$.

The above-chosen width of the layers is taken from the works [37, 38, 40].

The influence of various fluid flow controlling parameters like Darcy numbers, material parameter, viscosity ratio, etc. on the flow velocity, flow rate and shear stresses are discussed below.

5.1 Discussion on Flow Velocity and Micropolar Fluid Layer

The effect of middle layer on the velocity profile in different sections of horizontal porous channel is shown in Fig. 2. The parabolic nature of the velocity profile in the horizontal channel validates our result with the Poiseuille flow under the presence of constant pressure gradient. Therefore, the nature obtained for the flows in horizontal channel is in good agreement with the Poiseuille flow with no-slip boundary condition. The aim of this work is to observe the effect of the width of middle layer on the flows. It is clearly shown (Fig. 2) that flows through the middle porous layer of channel are higher in case $\alpha = 0.49$ and $\beta = 0.51$, i.e., the width of middle layer is lesser than the upper and lower porous layers of the channel.

The rate of increase in the velocity of micropolar fluid in the middle layer of the horizontal porous channel increases with the decrease in the width of micropolar fluid layer. It is also important to note that the velocity of Newtonian fluids in lower and upper regions of the horizontal porous channel is almost same when the width of middle layer is equal or not equal to the width of other two lower and upper layers. The same nature of the effect of

Fig. 2 Variation in velocity profile with the width of the middle layer when $Da_1 = 0.1 = Da_2 = Da_3$, $m = 1$, $P = -0.7$ and $K = 1$

thinner middle layer can be found in the works of Zaytoon et al. [37, 38].

5.2 Effect of Middle Layer Width, Darcy Number, Viscosity Ratio, Material Parameter on the Flow Rate

In this subsection, we have discussed the variation in the flow rate with middle layer width, Darcy number, viscosity ratio and material parameter. Figure 3a depicts the variation in flow rate with viscosity ratio and also with Darcy numbers Da_1, Da_2, Da_3 of three layers when the middle layer has equal width, i.e., when $\alpha = 1/3$ and $\beta = 2/3$.

From the above figure, we have concluded that the viscosity ratio and the volumetric flow rate in the horizontal channel increase together. Also, the flow rate is more in case where Darcy number of middle layers is greater than the Darcy numbers of other two layers. It is important to note that the rate of flow in channel increases rapidly for lower values of viscosity ratio ($m \leq 2$). It is also observed that the flow rate is almost equal for higher values of viscosity ratio when all the Darcy numbers are unequal and Darcy number of middle layers is less than the Darcy numbers of other two layers of the porous regions of the horizontal channel.

Figure 3b shows the variation in flow rate with viscosity ratio and also with permeability Da_1, Da_2, Da_3 of three layers when the middle layer is thicker than other layers, i.e., when $\alpha = 1/4$ and $\beta = 3/4$. Figure 3b shows that the dependency of flow rate on viscosity ratio for thick middle layer seems to be same in nature as in case of equal width of the layers, but the values of flow rate shown in Fig. 3b are higher than that shown in Fig. 3a. The variation in flow rate with viscosity ratio and permeabilities—Da_1, Da_2 and Da_3—of three layers, when the middle layer is thinner than other layers, i.e., when $\alpha = 0.49$ and $\beta = 0.51$, is shown in Fig. 3c. In this case, flow rate is higher when Darcy number of middle layer is less than other two layers. It is important to note that the variation in flow rate with all cases of Darcy number is almost constant except when Darcy number of middle layer is less than other two layers.

The changes observed in flow rate with respect to the material parameter of micropolar fluid for all three cases of the width of middle porous layer are shown in Fig. 3d. From this figure, it is noticed that the flow rate decreases with the increase in micropolarity parameter and seems to be constant in case of thin middle layer and lowest for thick middle layer.

The influence of Darcy number $Da_1\left(\lambda_1 = \frac{1}{\sqrt{Da_1}}\right)$ of upper porous layer on the flow rate for equal, thick and thin micropolar fluid layers is discussed in Fig. 3e–g. From these figures, we concluded that flow rate is decreasing with increasing values of parameter λ_1, i.e., with the decrease in Darcy numbers of upper porous layers.
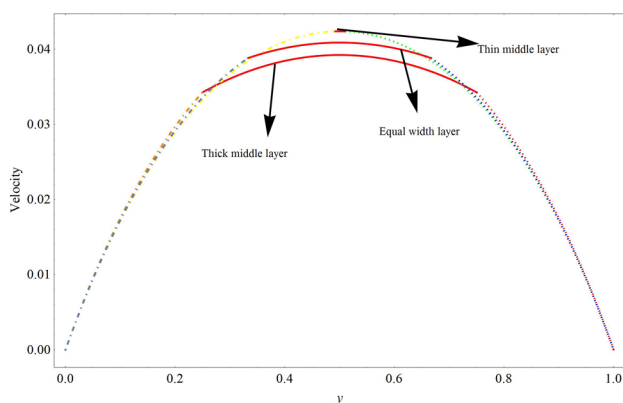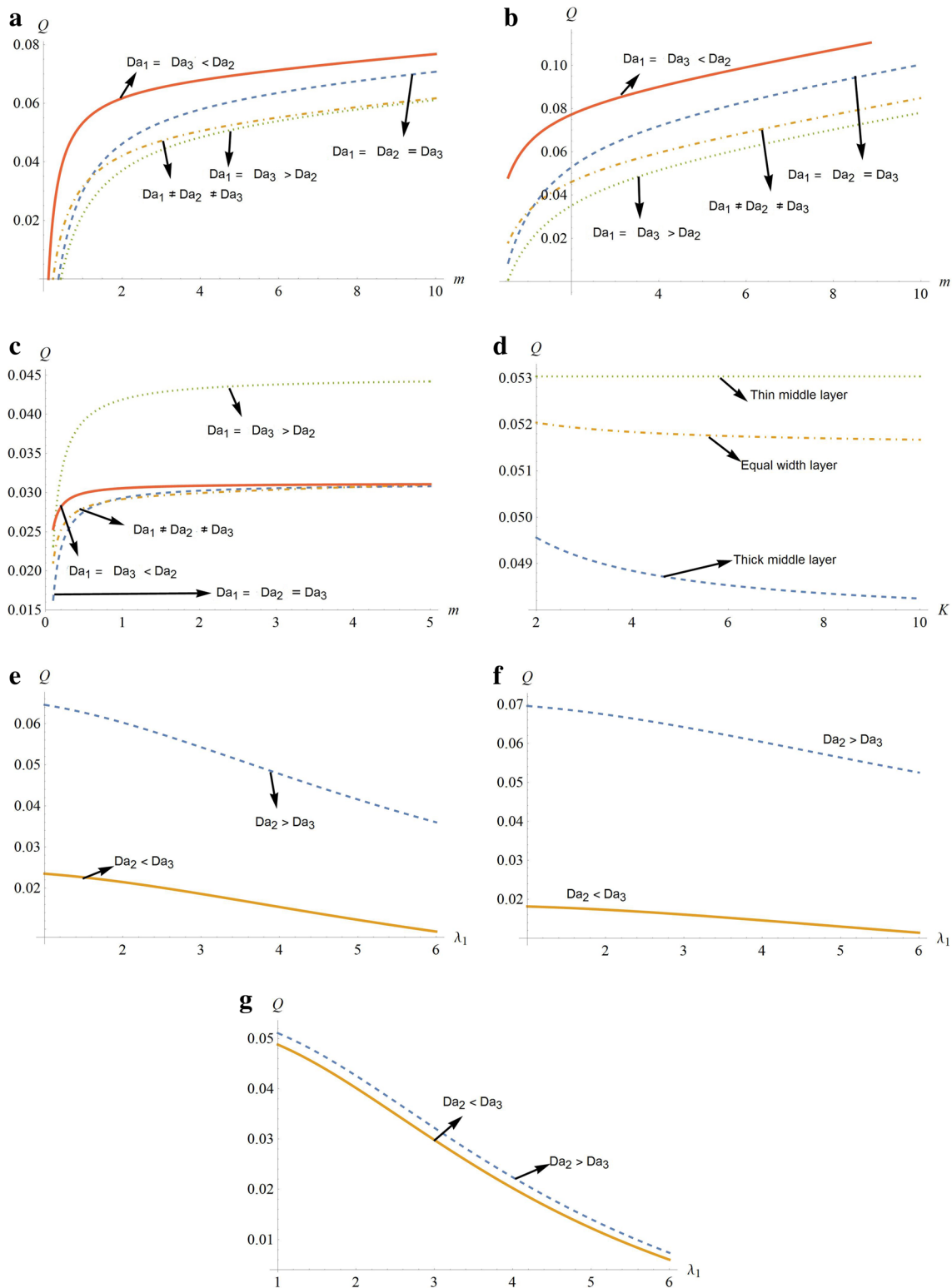
Fig. 3 a Variation in flow rate with viscosity ratio and Darcy numbers when $\alpha = 1/3$, $\beta = 2/3$, $P = -0.7$, $m = 1$ and $K = 1$. **b** Variation in flow rate with viscosity ratio and Darcy numbers when $\alpha = 1/4$, $\beta = 3/4$, $P = -0.7$ and $K = 1$. **c** Variation in flow rate with viscosity ratio and Darcy numbers when $\alpha = 0.49$, $\beta = 0.51$, $P = -0.7$ and $K = 1$. **d** Variation in flow rate with micropolarity parameter and transition layer when $P = -0.7$, $Da_1 = Da_2 = Da_3 = 1$ and $m = 1$. **e** Variation in flow rate with Darcy number when $P = -0.7$, $K = 1$, $\alpha = 1/3$, $\beta = 2/3$ and $m = 1$. **f** Variation in flow rate with Darcy number when $P = -0.7$, $K = 2$, $\alpha = 1/4$, $\beta = 3/4$ and $m = 1$. **g** Variation in flow rate with Darcy number when $P = -0.7$, $K = 1$, $\alpha = 0.49$, $\beta = 0.51$

Figure 3e–g shows that the value of flow rate is higher when Darcy number of middle layer is higher than the Darcy number of lower porous layer. The variation in flow rate with the parameter λ_1 for all types of middle layer is also given numerically in Table 1.

5.3 Effect of Middle Layer Width, Darcy Number, Micropolarity Parameter on the Velocity Profile of the Micropolar Fluid

The variation in the flow velocity of micropolar fluid in middle layer with middle layer's Darcy number for different widths of the middle layer is shown in Fig. 4a–c, when $Da_1 = Da_3 = 0.1$, $m = 1$, $K = 2$ and $P = -0.7$. From these figures, we concluded that the value of flow velocity of

Table 1 Variation in the flow rate with the reciprocal of Darcy number and width of middle layer when $P = -0.7$, $K = 2$ and $m = 1$

|	Flow rate					
	Equal width porous layer		Thin middle layer		Thick middle layer	
λ_1	$Da_3 > Da_2$	$Da_2 > Da_3$	$Da_3 > Da_2$	$Da_2 > Da_3$	$Da_3 > Da_2$	$Da_2 > Da_3$
1.0	0.0235	0.0646	0.0488	0.0511	0.0181	0.0696
1.2	0.0232	0.0639	0.0474	0.0497	0.0180	0.0692
1.5	0.0226	0.0627	0.0449	0.0473	0.0177	0.0686
1.8	0.0220	0.0613	0.0421	0.0446	0.0175	0.0679
2.0	0.0215	0.0603	0.0402	0.0426	0.0173	0.0674
2.5	0.0201	0.0574	0.0350	0.0374	0.0167	0.0659
3.0	0.0186	0.0543	0.0298	0.0322	0.0161	0.0642
3.5	0.0170	0.0510	0.0248	0.0271	0.0153	0.0623
4.0	0.0154	0.0478	0.0202	0.0224	0.0146	0.0603
4.5	0.0138	0.0446	0.0160	0.0180	0.0138	0.0584
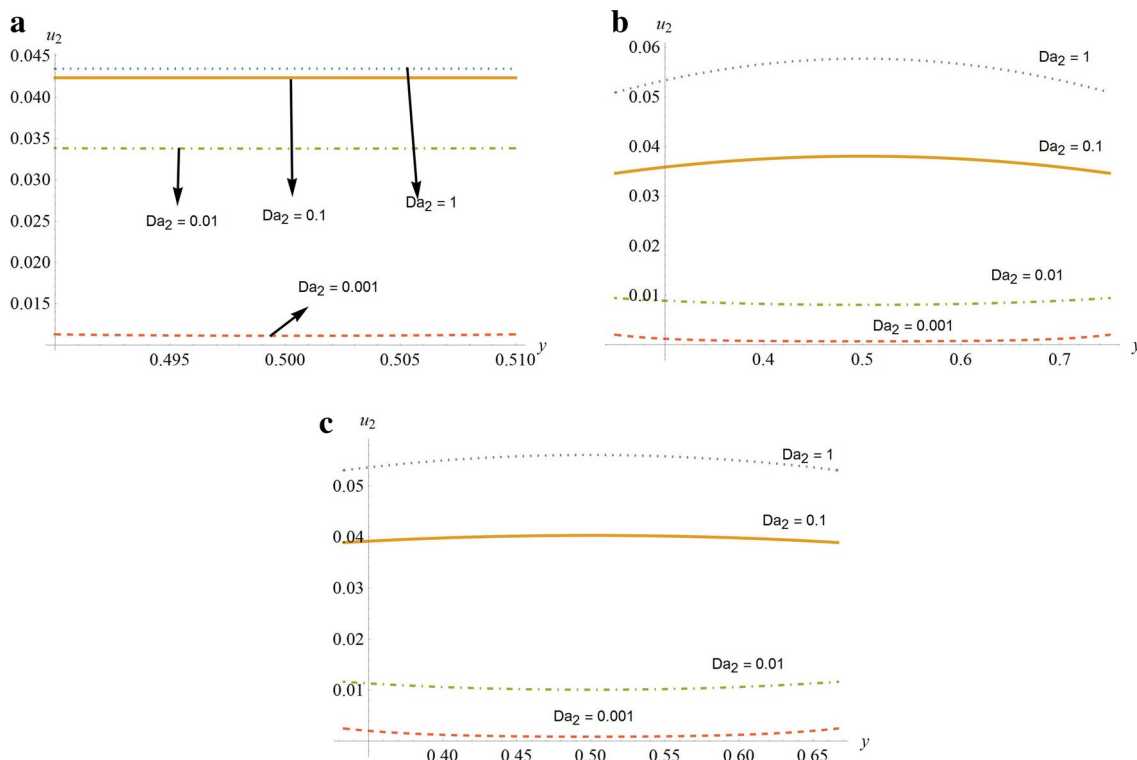
Fig. 4 **a** Variation in micropolar fluid flow velocity for thin middle layer. **b** Variation in micropolar fluid flow velocity for thick middle layer. **c** Variation in micropolar fluid flow velocity when width of all layers is equal

micropolar fluid in middle layer increases with the increase in middle layer's Darcy number.

For thin middle layer (Fig. 4a), the variation in flow velocity of micropolar fluid in middle layer is almost constant for particular value of the Da_2. It is important to note that the micropolar fluid velocity achieves the maximum value near the center of region-II for higher value of the middle layer's Darcy number $(Da_2 > 0.1)$; however, it achieves the minimum value near the center of region-II for low value of the middle layer's Darcy number $(Da_2 < 0.01)$ (Fig. 4b, c).

From the theory of micropolar fluid discussed in Eringen [57], it is known that the micropolar fluid can be reduced to the Newtonian fluid by taking $\kappa \to 0$ (in the absence of micro-rotational velocity). Thus, our model can reduce to the flow of immiscible Newtonian fluids through the composite porous layered channel with movable interfaces by taking $\kappa \to 0$ in Eq. (11). The similar type of problem with variable and generalized variable permeability had been solved by Zaytoon et al. [37, 38].

In this case, the governing equation for the flow of fluid in region-II will be as follows:

$$\frac{d^2 u_2}{dy^2} - \frac{u_2}{Da_2} = mP. \tag{36}$$

The expression for the velocity of Newtonian fluid in region-II can be obtained by solving the above equation which is given below:

$$u_2(y) = B_1 \exp(\lambda_2 y) + B_2 \exp(-\lambda_2 y) - \frac{mP}{\lambda_2^2}, \tag{37}$$

where $\lambda_2 = \frac{1}{\sqrt{Da_2}}$ and B_1, B_2 are arbitrary constants which can be obtained by using the above suitable boundary conditions.

The variation in Newtonian fluid velocity in region-II with middle layer's Darcy number for different widths of the middle layer and its comparison with velocity of micropolar fluid in middle layer is shown in Fig. 5a–c, when $Da_1 = Da_2 = Da_3 = 0.1$, $m = 0$, $K = 1$ and $P = -0.7$. The dotted lines show the flow of Newtonian–Newtonian–Newtonian flow through the composite porous layers, while the solid lines show Newtonian–micropolar–Newtonian flow model through the composite porous layers.

Figure 5 shows that the nature of variation in Newtonian fluid velocity in region-II with middle layer's Darcy number agrees with the variation in Newtonian fluid velocity in region-II with middle layer's Darcy number as discussed in the work of Zaytoon et al. [37, 38]. Figure 5 shows that the velocity of micropolar fluid inside the middle layer is less as compared to the velocity of Newtonian fluid.
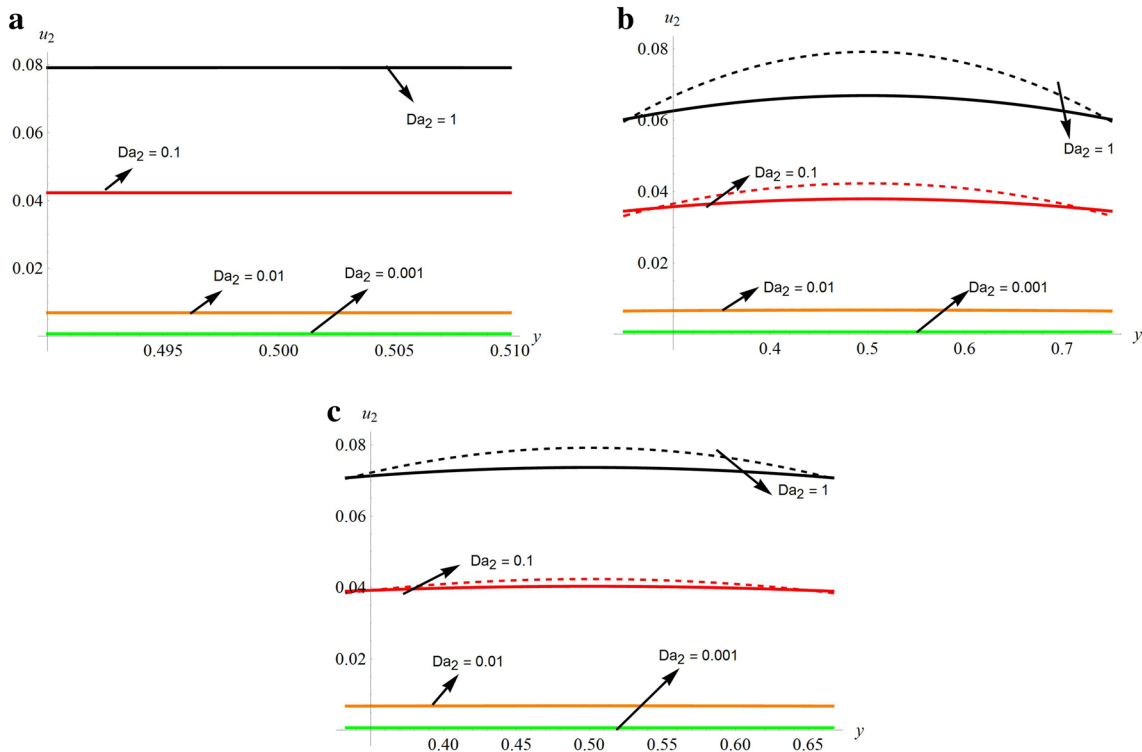

Fig. 5 a Variation in micropolar fluid flow velocity for thin middle layer. b Variation in micropolar fluid flow velocity for thick middle layer. c Variation in micropolar fluid flow velocity when width of all layers is equal
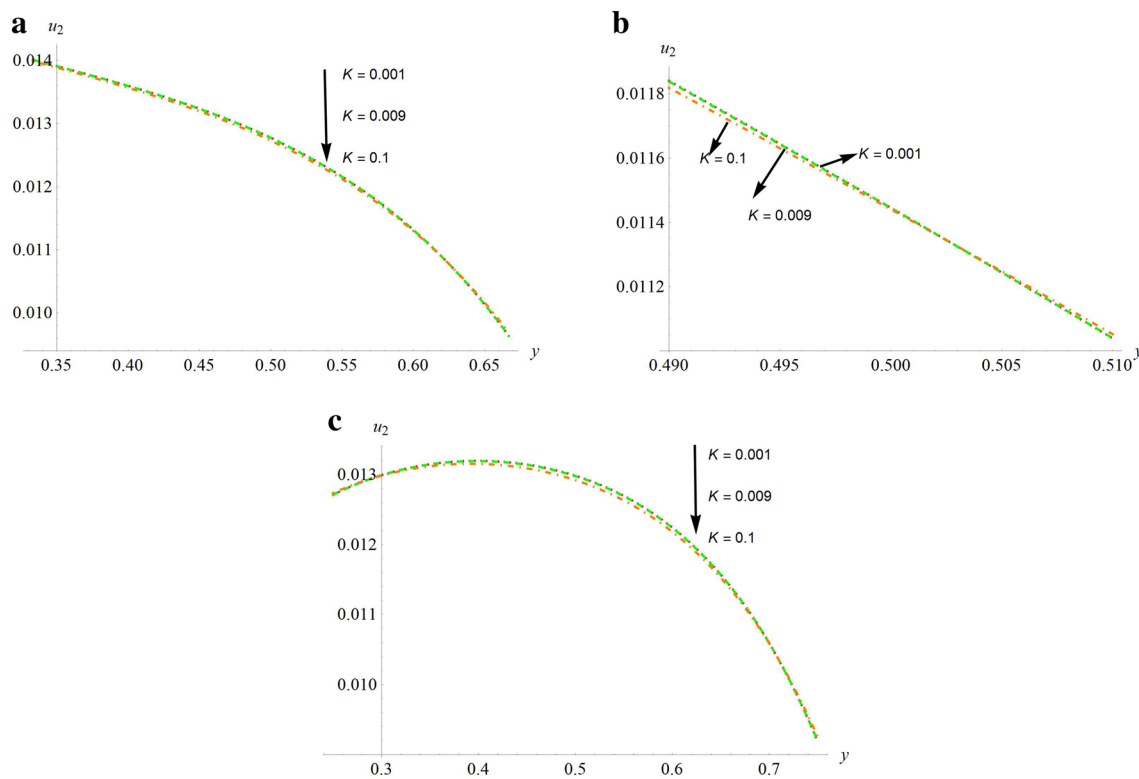
Fig. 6 **a** Variation in micropolar fluid flow velocity with material parameter when width of all layers is equal. **b** Variation in micropolar fluid flow velocity with material parameter when middle layer is thin. **c** Variation in micropolar fluid flow velocity with material parameter when middle layer is thick

Figure 6a, b and c represents the variation in micropolar fluid velocity, in middle layer with respect to micropolarity parameter for different middle layer's widths, i.e., equal width, thin and thick, respectively, when $m = 1$ and $P = -0.7$. Also, in this subsection, we have taken the different permeabilities of all three porous layers, i.e., $Da_1 = 0.01$, $Da_2 = 0.02$ and $Da_3 = 0.03$.

Figure 6 shows that the flow velocity of micropolar fluid in middle layer decreases with the increasing values of the material parameter K. Since material parameter is only the parameter for describing the rotational property of micropolar fluid, there will be no effect on the velocity of the Newtonian fluids passing in region-I and region-III, respectively.

Table 2 Variation in the shearing stress at the interfaces and interfacial velocity with Darcy number and width of middle layer when $P = -0.7$, $K = 1$, $Da_1 = Da_2 = Da_3 = Da$ and $m = 1$

$Da \rightarrow$		1	0.1	0.01	0.001
$\tau_{xy}(\beta)$	Equal width layers	-0.1044	-0.0497	-0.00269	-6.847×10^{-7}
	Thick middle layer	-0.15832	-0.0811	-0.00657	-9.549×10^{-6}
	Thin middle layer	-0.00621	-0.00276	-0.000094	-1.960×10^{-9}
$\tau_{xy}(\alpha)$	Equal width layers	-0.1044	-0.0497	-0.00269	-6.847×10^{-7}
	Thick middle layer	-0.15832	-0.0811	-0.00657	-9.549×10^{-6}
	Thin middle layer	-0.00621	-0.00276	-0.000094	-1.960×10^{-9}
$u_1(\beta)$	Equal width layers	0.07073	0.03881	0.00677	0.000699
	Thick middle layer	0.06009	0.034226	0.00650	0.0006998
	Thin middle layer	0.07920	0.04235	0.006905	0.0007
$u_3(\alpha)$	Equal width layers	0.07073	0.03881	0.00677	0.000699
	Thick middle layer	0.06009	0.034226	0.00650	0.0006998
	Thin middle layer	0.07920	0.04235	0.006905	0.0007

Table 3 Variation in the shearing stress at the interfaces and interfacial velocity with viscosity ratio and middle layer's width when $P = -0.7$, $K = 2$, $Da_1 = 1$, $Da_2 = 1$ and $Da_3 = 1$

$m \rightarrow$		0.1	0.5	1	1.5	2	5	10
$\tau_{xy}(\beta)$	Equal width layers	-0.0356	-0.0939	-0.1045	-0.1083	-0.1103	-0.1139	-0.1151
	Thick middle layer	-0.0752	-0.1455	-0.1588	-0.1636	-0.1661	-0.1706	-0.1722
	Thin middle layer	0.0006	-0.0054	-0.0062	-0.0065	-0.0066	-0.0068	-0.0069
$\tau_{xy}(\alpha)$	Equal width layers	0.0356	0.0939	0.1045	0.1083	0.1103	0.1139	0.1151
	Thick middle layer	0.0752	0.1455	0.1588	0.1636	0.1661	0.1706	0.1722
	Thin middle layer	-0.0006	0.0054	0.0063	0.0065	0.0066	0.0068	0.0069
$u_1(\beta)$	Equal width layers	0.0486	0.0674	0.0708	0.0720	0.0726	0.0738	0.0742
	Thick middle layer	0.0397	0.0569	0.0602	0.0614	0.0620	0.0631	0.0635
	Thin middle layer	0.0761	0.0788	0.0792	0.0793	0.0794	0.0795	0.0796
$u_3(\alpha)$	Equal width layers	0.0486	0.0674	0.0708	0.0720	0.0726	0.0738	0.0742
	Thick middle layer	0.0397	0.0569	0.0602	0.0614	0.0620	0.0631	0.0635
	Thin middle layer	0.0761	0.0788	0.0792	0.0793	0.0794	0.0795	0.0796

5.4 Effect of Middle Layer, Viscosity Ratio and Transition Layer's Darcy Number on Velocities and Shearing Stress at Two Interfaces of Horizontal Channel

The effect of different Darcy numbers of the middle layer on the interfacial velocity and shearing stress is given numerically in Table 2. It is observed that the interfacial velocity and shearing stress decrease with the decrease in the Darcy number of middle porous layer. To validate our results with previously published work (Zaytoon et al. [37, 38, 40]), here we assumed that the Darcy number of each layer is same, i.e., $Da_1 = Da_2 = Da_3 = Da$. Table 2 shows that the nature of variation in the interfacial velocity and shearing stress with the Darcy number agree with the nature of variation in the interfacial velocity and shearing stress with the Darcy number as discussed in the work of Zaytoon et al. [37, 38, 40].

Table 2 shows that the interfacial shearing stress is greater for the thicker middle layer as compared to other two cases of middle layer and the interfacial velocity is high for thinner middle layer as compared to thick middle layer and equal width layer. The effect of viscosity ratio m on the interfacial velocity and shearing stress is given numerically in Table 3.

It is observed that shearing stress and velocity at micropolar–Newtonian interfaces increase with the increase in the values of the viscosity ratio. Table 3 also provides another important fact that the variation in interfacial velocity rate and shearing stress is very slow for higher values of viscosity ratio m.

6 Conclusions

In this work, we have analytically solved the problem of micropolar–Newtonian fluid flow through horizontal porous channel, in which each layer's width can be varied. The problem is modeled in such a manner that it could be applicable for the medical as well as industrial purposes. All the three porous layers are assumed to have different permeabilities. The mean flow velocity, shear stress at the interfaces, velocities at the interfaces and the flow velocity of each fluid in their respective region have been obtained. The effect of the middle layer's width on the flows has been reported. It is observed that when the middle layer is thin then the flow velocity in the channel is higher. The discussed result validates our work with the works [35, 37, 38]. The rotational property of micropolar fluid deaccelerates the flow velocity in each case of the widths of the middle layer. Also, it is seen that when the three porous layers has different permeabilities then the flow velocity is found to be higher in the channel. The effect of middle layer's Darcy number and viscosity ratio on the interfacial velocity and shearing stress is also discussed and concluded that the interfacial shearing stress increases by increasing the thickness of the middle layer and interfacial velocity decreases by decreasing the thickness of the middle layer.

References

1. Yuan, S.W.: Foundations of Fluid Mechanics. Prentice Hall, London (1970)
2. Coutelieris, F.A.; Delgado, J.M.P.Q.: Transport Processes in Porous Media. Springer, Berlin (2012)
3. Yadav, P.K.; Deo, S.; Yadav, M.K.; Filippov, A.: On hydrodynamic permeability of a membrane built up by porous deformed spheroidal particles. Colloid J. **75**(5), 611–622 (2013)
4. Yadav, P.; Tiwari, A.; Singh, P.: Hydrodynamic permeability of a membrane built up by spheroidal particles covered by porous layer. Acta Mech. **229**(4), 1869–1892 (2018)

5. Yadav, P.; Tiwari, A.; Deo, S.; Filippov, A.; Vasin, S.: Hydrodynamic permeability of membranes built up by spherical particles covered by porous shells: effect of stress jump condition. Acta Mech. **215**, 193–209 (2010)

6. Hamdan, M.H.: Single-phase flow through porous channels a review of flow models and channel entry conditions. Appl. Math. Comput. **62**, 203–222 (1994)

7. Rudraiah, N.: Coupled parallel flows in a channel and a bounding porous medium of finite thickness. J. Fluids Eng. **107**(3), 322–329 (1985)

8. Kaviany, M.: Laminar flow through a porous channel bounded by isothermal parallel plates. Int. J. Heat Mass Transf. **28**(4), 851–858 (1985)

9. Chamkha, A.J.: On laminar hydromagnetic mixed convection flow in a vertical channel with symmetric and asymmetric wall heating conditions. Int. J. Heat Mass Transf. **45**(12), 2509–2525 (2002)

10. Umavathi, J.C.; Kumar, J.P.; Chamkha, A.J.; Pop, I.: Mixed convection in a vertical porous channel. Trans. Porous Med. **61**(3), 315–335 (2005)

11. Umavathi, J.C.; Chamkha, A.J.; Sridhar, K.S.R.: Generalized plain Couette flow and heat transfer in a composite channel. Trans. Porous Med. **85**(1), 157–169 (2010)

12. Umavathi, J.C.; Chamkha, A.J.; Mateen, A.; Al-Mudhaf, A.: Oscillatory flow and heat transfer in a horizontal composite porous medium channel. Int. J. Heat Technol. **25**, 75–86 (2006)

13. Umavathi, J.C.; Chamkha, A.J.; Mateen, A.; Al-Mudhaf, A.: Unsteady oscillatory flow and heat transfer in a horizontal composite porous medium channel. Nonlinear Anal. Model. Control **14**(3), 397–415 (2009)

14. Chamkha, A.J.; Khaled, A.R.A.: Similarity solutions for hydromagnetic mixed convection heat and mass transfer for Hiemenz flow through porous media. Int. J. Numer. Methods Heat Fluid Flow **10**(1), 94–115 (2000)

15. Ismael, M.A.; Pop, I.; Chamkha, A.J.: Mixed convection in a lid-driven square cavity with partial slip. Int. J. Therm. Sci. **82**, 47–61 (2014)

16. Chamkha, A.J.: Double-diffusive convection in a porous enclosure with cooperating temperature and concentration gradients and heat generation or absorption effects. Numer. Heat Transf. Part A Appl. **41**(1), 65–87 (2002)

17. Magyari, E.; Chamkha, A.J.: Exact analytical results for the thermosolutal MHD Marangoni boundary layers. Int. J. Therm. Sci. **47**(7), 848–857 (2008)

18. Yadav, P.K.: Slow motion of a porous cylindrical shell in a concentric cylindrical cavity. Meccanica **48**(7), 1607–1622 (2013)

19. Tiwari, A.; Yadav, P.K.; Singh, P.: Stokes flow through assemblage of non-homogeneous porous cylindrical particles using cell model technique. Natl. Acad. Sci. Lett. **41**(1), 53–57 (2018)

20. Vafai, K.; Thiyagaraja, R.: Analysis of flow and heat transfer at the interface region of a porous medium. Int. J. Heat Mass Transf. **30**(7), 1391–1405 (1987)

21. Sahraoui, M.; Kaviany, M.: Slip and no-slip velocity boundary conditions interface of porous, plain -media. Int. J. Heat Mass Transf. **35**(4), 927–943 (1992)

22. Ansari, I.; Deo, S.: Effect of magnetic field on the two immiscible viscous fluids flow in a channel filled with porous medium. Natl. Acad. Sci. Lett. **40**(3), 211–214 (2017)

23. Umavathi, J.C.; Chamkha, A.J.; Mateen, A.; Al-Mudhaf, A.: Unsteady two-fluid flow and heat transfer in a horizontal channel. Heat Mass Transf. **42**(2), 81 (2005)

24. Umavathi, J.C.; Mateen, A.; Chamkha, A.J.; Al Mudhaf, A.: Oscillatory hartmann two-fluid flow and heat transfer in a horizontal channel. Int. J. Appl. Mech. Eng. **26**(4), 155–178 (2006)

25. Umavathi, J.C.; Chamkha, A.J.; Manjula, M.H.; Al-Mudhaf, A.F.: Radiative heat transfer of a two-fluid flow in a vertical porous stratum. Int. J. Fluid Mech. Res. **35**(6), 510–543 (2008)

26. Umavathi, J.C.; Chamkha, A.J.; Abdul, M.; Kumar, J.P.: Unsteady magnetohydroynamic two fluid flow and heat transfer in a horizontal channel. Int. J. Heat Technol. **26**, 121–133 (2008)

27. Umavathi, J.C.; Kumar, J.P.; Chamkha, A.J.: Convective flow of two immiscible viscous and couple stress permeable fluids through a vertical channel. Turk. J. Eng. Environ. Sci. **33**(4), 221–244 (2010)

28. Chamkha, A.J.: Unsteady laminar hydromagnetic fluid–particle flow and heat transfer in channels and circular pipes. Int. J. Heat Fluid Flow **21**(6), 740–746 (2000)

29. Allan, F.M.; Hamdan, M.H.: Fluid mechanics of the interface region between two porous layers. Appl. Math. Comput. **128**(1), 37–43 (2002)

30. Ford, R.A.; Hamdan, M.H.: Coupled parallel flow through composite porous layers. Appl. Math. Comput. **97**, 261–271 (1998)

31. Yadav, P.K.: Motion through a non-homogeneous porous medium: hydrodynamic permeability of a membrane composed of cylindrical particles. Eur. Phys. J. Plus. **133**(1), 1–26 (2018)

32. Hamdan, M.H.; Kamel, M.T.; Siyyam, H.I.: A permeability function for Brinkman's equation. In: Mathematical Methods, Computational Techniques and Intelligent Systems. pp. 198–205 (2009)

33. Awartani, M.M.; Hamdan, M.H.: Fully developed flow through a porous channel bounded by flat plates. Appl. Math. Comput. **169**(2), 749–757 (2005)

34. Chandesris, M.; Jamet, D.: Boundary conditions at a planar fluid-porous interface for a Poiseuille flow. Int. J. Heat Mass Transf. **49**, 2137–2150 (2006)

35. Nield, D.A.; Kuznetsov, A.V.: The effect of a transition layer between a fluid and a porous medium: shear flow in a channel. Transp. Porous Media **78**(3), 477–487 (2009)

36. Umavathi, J.C.; Chamkha, A.J.; Manjula, M.H.; Al-Mudhaf, A.: Flow and heat transfer of a couple-stress fluid sandwiched between viscous fluid layers. Can. J. Phys. **83**(7), 705–720 (2005)

37. Abu Zaytoon, M.S.; Alderson, T.L.; Hamdan, M.H.: Flow through layered media with embedded transition porous layer. Int. J. Enhanc. Res. Sci. Technol. Eng. **5**(4), 9–26 (2016)

38. Abu Zaytoon, M.S.; Alderson, T.L.; Hamdan, M.H.: Flow through a layered porous configuration with generalized variable permeability. Int. J. Enhanc. Res. Sci. Tchnol. Eng. **5**(6), 1–22 (2016)

39. Abu Zaytoon, M.S.; Alderson, T.L.; Hamdan, M.H.: Flow over a Darcy porous layer of variable permeability. J. Appl. Math. Phys. **4**(1), 86–99 (2016)

40. Abu Zaytoon, M.S.; Alderson, T.L.; Hamdan, M.H.: Flow through a variable permeability Brinkman porous core. J. Appl. Math. Phys. **4**(4), 766–778 (2016)

41. Alzahrani, S.M.; Gadoura, I.; Hamdan, M.H.: A note on the flow of a fluid with pressure-dependent viscosity through a porous medium with variable permeability. J. Mod. Technol. Eng. **2**(1), 21–33 (2017)

42. Umavathi, J.C.; Kumar, J.P.; Chamkha, A.J.: Flow and heat transfer of a micropolar fluid sandwiched between viscous fluid layers. Can. J. Phys. **86**(8), 961–973 (2008)

43. Kumar, J.P.; Umavathi, J.C.; Chamkha, A.J.; Pop, I.: Fully-developed free-convective flow of micropolar and viscous fluids in a vertical channel. Appl. Math. Model. **34**(5), 1175–1186 (2010)

44. Umavathi, J.C.; Chamkha, A.J.; Shekar, M.: Flow and heat transfer of two micropolar fluids separated by a viscous fluid layer. Int. J. Microsc. Nanosc. Therm. Fluid Transp. Phenom. **5**(1), 23 (2014)

45. Damseh, R.A.; Al-Odat, M.Q.; Chamkha, A.J.; Shannak, B.A.: Combined effect of heat generation or absorption and first-order chemical reaction on micropolar fluid flows over a uniformly stretched permeable surface. Int. J. Therm. Sci. **48**(8), 1658–1663 (2009)

46. Magyari, E.; Chamkha, A.J.: Combined effect of heat generation or absorption and first-order chemical reaction on micropolar fluid

flows over a uniformly stretched permeable surface: the full analytical solution. Int. J. Therm. Sci. **49**(9), 1821–1828 (2010)

47. Yadav, P.K.; Jaiswal, S.; Sharma, B.D.: A mathematical model of micropolar fluid in two-phase immiscible fluid flow through porous channel. Appl. Math. Mech. **39**(7), 1–17 (2018)

48. Yadav, P.K.; Jaiswal, S.: Influence of an inclined magnetic field on the Poiseuille flow of immiscible micropolar-Newtonian fluids in the porous medium. Can. J. Phys. **96**, 1016–1028 (2018)

49. Yadav, P.K.; Jaiswal, S.; Asim, T.; Mishra, R.: Influence of magnetic field on the flow of micropolar fluid sandwiched between two Newtonian fluid layers through porous medium. Eur. Phys. J. Plus. **133**, 247–260 (2018)

50. Al-Mutairi, S.M.; Abu-Khamsin, S.A.; Hossain, M.E.: A new rigorous mathematical model to describe immisicble CO_2-oil flow in porous media. J. Porous Media. **17**(5), 421–429 (2014)

51. Siddique, M.H.; Bellary, S.A.I.; Samad, A.; Kim, J.H.: Experimental and Numerical investigation of the performance of a centrifugal pump when pumping water and light crude oil. Arab. J. Sci. Eng. **42**(11), 4605–4615 (2017)

52. Brinkman, H.C.: A Calculation of the viscous force exerted by a flowing fluid on a dense swarm of particles. Appl. Sci. Res. **2**, 155–161 (1951)

53. Darcy, H.: Les fontaines publique de la ville de Dijon. Dalmont, Paris (1856)

54. Liu, S.; Masliyah, J.H.: Single Fluid Flow in Porous Media. Chem. Eng. Commun. **148**(1), 653–732 (1996)

55. Nield, D.A.; Bejan, A.: Convection in Porous Media, 3rd edn. Springer, New York (2006)

56. Eringen, A.C.: Simple microfluids. Int. J. Eng. Sci. **2**, 205–217 (1964)

57. Eringen, A.C.: Theory of micropolar fluids. J. Math. Mech. **16**, 1–18 (1966)

58. Lukaszewicz, G.: Micropolar Fluids Theory and Applications. Springer, Berlin (2004)

59. Ahmadi, G.: Self-similar solution of incompressible micropolar boundary layer flow over a semi-infinite plate. Int. J. Eng. Sci. **14**(7), 639–646 (1976)